

# LabTOP: A Unified Model for Lab Test Outcome Prediction on Electronic Health Records

Sujeong Im\*

Jungwoo Oh\*

Edward Choi

KAIST, Republic of Korea

SUJEONGIM@KAIST.AC.KR

OJW0123@KAIST.AC.KR

EDWARDCHOI@KAIST.AC.KR

## Abstract

Lab tests are fundamental for diagnosing diseases and monitoring patient conditions. However, frequent testing can be burdensome for patients, and test results may not always be immediately available. To address these challenges, we propose **Lab Test Outcome Predictor (LabTOP)**, a unified model that predicts lab test outcomes by leveraging a language modeling approach on EHR data. Unlike conventional methods that estimate only a subset of lab tests or classify discrete value ranges, LabTOP performs continuous numerical predictions for a diverse range of lab items. We evaluate LabTOP on three publicly available EHR datasets and demonstrate that it outperforms existing methods, including traditional machine learning models and state-of-the-art large language models. We also conduct extensive ablation studies to confirm the effectiveness of our design choices. We believe that LabTOP will serve as an accurate and generalizable framework for lab test outcome prediction, with potential applications in clinical decision support and early detection of critical conditions.

**Data and Code Availability** This paper uses the three EHR datasets, MIMIC-IV (Johnson et al., 2023), eICU (Pollard et al., 2018), and HiRID (Hyland et al., 2020), which are publicly available on the PhysioNet repository (Johnson et al., 2020; Pollard et al., 2019; Faltys et al., 2021). More details about datasets can be found at Section 4.1. Our implementation code can be accessed at this repository.<sup>1</sup>

**Institutional Review Board (IRB)** This research does not require IRB approval.

## 1. Introduction

Electronic Health Records (EHR) are essential to modern healthcare systems, serving as comprehensive databases of patient data, including treatments, clinical interventions, and lab test results (Gunter and Terry, 2005). These records provide a longitudinal view of a patient’s medical history, allowing for the tracking of individual health trends (Kruse et al., 2017). Among them, lab test results play a particularly important role by capturing numerical changes in key biomarkers, such as blood glucose and creatinine. These results reflect a patient’s physiological and pathological state, supporting the management of disease and the assessment of treatment efficacy (Sikaris, 2017; Cabalar et al., 2024).

Despite their clinical importance, conducting lab tests often faces challenges in real-world settings. For instance, the need for frequent lab tests in unstable patients conflicts with the increased distress they experience from repeated invasive procedures, creating a trade-off between clinical necessity and patient burden (Ambasta et al., 2019; Zhi et al., 2024). Additionally, some tests often take significant time to obtain results, making it difficult to assess the patient’s condition promptly (Shiferaw and Yismaw, 2019). As a result, there are limitations in comprehensively assessing a patient’s condition from multiple perspectives through various lab tests, forcing healthcare providers to rely solely on the available test results to make clinical judgments. This challenge highlights the need for methods to estimate lab test results without conducting the actual tests, allowing healthcare providers to understand a patient’s condition comprehensively through the predicted lab test results.

Meanwhile, the advancement of machine learning has greatly contributed to healthcare for several clinical prediction tasks such as readmission, mortal-

\* These authors contributed equally

1. <https://github.com/sujeongim/LabTOP>

ity risk, and length of hospital stay (Song et al., 2018; Xiao et al., 2018; Hur et al., 2022, 2023; Kim et al., 2023; Wornow et al., 2023; Renc et al., 2024). While previous studies have demonstrated the value of lab test data in supporting clinical decisions, efforts to estimate various lab test results within a single unified model have been limited. Notably, most prior studies approach lab test outcome prediction by classifying discrete levels of a small subset of selected lab items (Hur et al., 2023; Kim et al., 2023; Wornow et al., 2023). Even among studies that attempt to estimate continuous values, they are specifically designed for only a few selected lab tests rather than whole set of lab items (Zhi et al., 2024; Jiang et al., 2024; Duan et al., 2020; Liu et al., 2023; Fu et al., 2023; Langarica et al., 2024). On the other hand, some works on irregularly sampled time-series models have explored the prediction of multiple lab measurements using neural ODE-based approaches (Rubanova et al., 2019; Schirmer et al., 2022). These methods estimate multiple lab values within a unified framework; however, they primarily focus on modeling the dynamics of lab test results alone, without incorporating the broader medical events present in EHRs, such as medications and input events. This narrow focus limits their practical applicability in clinical settings, where precise numerical predictions for a broader range of lab test results can facilitate early intervention and support more informed clinical decision-making across diverse medical conditions.

To address these limitations, we propose **Lab Test Outcome Predictor (LabTOP)**, a novel method for predicting a diverse range of lab test outcomes based on a patient’s medical history within a single unified model. Inspired by autoregressive models widely used in Natural Language Processing (Radford et al., 2018, 2019), we leverage language modeling paradigm to predict numeric values in an autoregressive manner, instead of regressing each lab test value separately. This approach enables us to build a unified model capable of predicting outcomes for multiple lab items within a single framework, without requiring us to train a separate model for each lab item. Furthermore, unlike prior approaches, LabTOP is designed to estimate continuous lab test measurements across a wide spectrum of biomarkers, offering greater granularity and broader applicability in clinical practice. The main contributions of this work can be summarized as follows:

- We propose LabTOP, a new model that estimates continuous values for a wide range of lab test measurements given the patient’s previous medical history. To the best of our knowledge, this is the first comprehensive approach to predict various lab test results within a single unified model trained on EHR data.
- LabTOP outperforms existing approaches, including a recent large language model (LLM), across three publicly available datasets. This demonstrates the generalizability of our method to diverse patient populations and clinical contexts.
- Considering the time-series characteristics of EHR data where each patient can be represented as a sequence of medical events, we conduct ablation studies to explore the best way to represent the time and numeric features of medical events for the model. We believe these experiments will provide valuable insights into effectively modeling EHR data.

## 2. Related Works

### Predicting clinical outcomes using EHR data

Previous machine learning models leveraging EHR data have primarily focused on predicting clinical outcomes, such as readmission, mortality risk, and length of stay (Song et al., 2018; Xiao et al., 2018; Hur et al., 2022, 2023; Kim et al., 2023; Wornow et al., 2023; Renc et al., 2024). Among them, Song et al. (2018) introduced the *SANd*, employing Transformer architecture (Vaswani, 2017) to predict in-hospital mortality and length of hospital stay. They constructed the input embeddings based on structured clinical codes (e.g., ICD, LOINC, RxNorm) to process EHR data, which makes it difficult to process multiple EHRs with different schemas within a single model. To address these challenges, Hur et al. (2022) proposed a text-based embedding approach (DescEmb) to represent EHR events using descriptive text rather than codes, showing superior performances compared to the code-based approach. Based on this text-based approach, GenHPF (Hur et al., 2023) extended it by incorporating multi-task learning to handle various predictive tasks simultaneously. Furthermore, REMed (Kim et al., 2023) integrated an event-retriever module into this framework to selectively extract relevant events with target tasks, en-

suring that only the important events contribute to the final predictions.

**Generative models for EHR data** In addition to the studies employing discriminative models for predictive tasks, generative approaches have also been explored for modeling EHR data. Specifically, MedGPT (Kraljevic et al., 2021) adopted the GPT-2 architecture (Radford et al., 2019) to predict next SNOMED-CT disorder concept given the patient’s previous history of disorders. Although this work utilized only the disorder concepts instead of a comprehensive set of clinical events in EHR, they demonstrated the potential of generative methods for simulating patient trajectories and predicting future clinical events. In addition, ETHOS (Renc et al., 2024) employed a generative approach based on language modeling to simulate clinical scenarios using a structured EHR data. Similar to the code-based approach, they converted each medical event into 1 to 7 tokens to construct the input sequence for the Transformer (Vaswani, 2017), and trained the model to predict every next token given the prior sequences to simulate the clinical outcomes of the patient, such as whether the patient will die or not (*i.e.*, mortality prediction).

**Lab test outcome prediction** Although previous studies have significantly advanced the field of machine learning for healthcare, only a few of them have addressed the direct estimation of continuous values for various lab tests within a single unified model. For example, there have been attempts to estimate multiple lab values within a unified framework using neural ODE-based approaches (Rubanova et al., 2019; Schirmer et al., 2022). However, a key limitation of these approaches is that they only model lab test values in isolation, without incorporating other essential patient events such as medications, interventions, and clinical inputs that may significantly influence lab test dynamics. Instead, most of previous studies have explored the prediction of lab test results by designing a specific model for only a few selected lab items or classifying discrete levels of selected lab items, such as normal or abnormal ranges. For example, HgbNet (Zhi et al., 2024) employed an attention-based LSTM model to estimate hemoglobin levels, while Jiang et al. (2024) presented a probabilistic model using NGBoost (Duan et al., 2020) to predict expected values of several lab items, such as wbc and hemoglobin. Similarly, several works (Liu et al., 2023; Fu et al., 2023; Langarica et al., 2024)

attempted to estimate glucose values using machine learning or deep learning approach. However, these approaches are specifically designed for a small subset of lab tests, making it challenging to generalize across diverse clinical measurements.

Meanwhile, GenHPF (Hur et al., 2023) and REMed (Kim et al., 2023) formulated this task as classifying the discrete level of values for several selected lab items. Although these works have shown high performances on the defined task, their predictions remain limited in terms of extensibility and granularity. First, they rely on predefined level thresholds for each lab item, determined through domain knowledge, which makes it difficult to extend the approach to encompass all lab items recorded in the EHR database. Second, as the task is defined within a fixed prediction window (*e.g.*, predicting average levels of lab items in the next 12 hours given the first 12 hours), these models lack granularity in providing immediate estimations of lab test results, which is critical for clinical scenarios where timely and dynamic predictions are necessary to inform urgent decisions.

### 3. Methods

#### 3.1. Preliminaries

In EHR data, patient medical events that occur in a hospital, such as lab tests and prescriptions, are recorded in a structured format. Thus, we can represent a patient  $P$  as a sequence of medical events  $[\mathcal{M}_1, \dots, \mathcal{M}_N]$ , where  $N$  is the total number of medical events, and  $\mathcal{M}_i$  is the  $i$ -th medical event for the patient. Each medical event typically includes a timestamp, medical event codes (*e.g.*, ICD, LOINC, RxNorm), a numerical value, and its corresponding unit of measurement. Accordingly, the  $i$ -th medical event  $\mathcal{M}_i$  can be represented as a 5-tuple of event features  $(t_i, e_i, c_i, v_i, u_i)$ , where  $t_i$  represents the timestamp of the event,  $e_i$  stands for the type of the event (*e.g.*, “labevent”, “prescription”),  $c_i$  is the corresponding medical code (*e.g.*, “2160-0”),  $v_i$  denotes the measured values (*e.g.*, 1.2), and  $u_i$  is the associated unit of measurement (*e.g.*, mg/dL). The detailed definitions of these event features are described in the following section, as well as depicted in Figure 1.

#### 3.2. Preprocessing

**Textual representation of medical events** Unlike conventional methods that directly embed med-

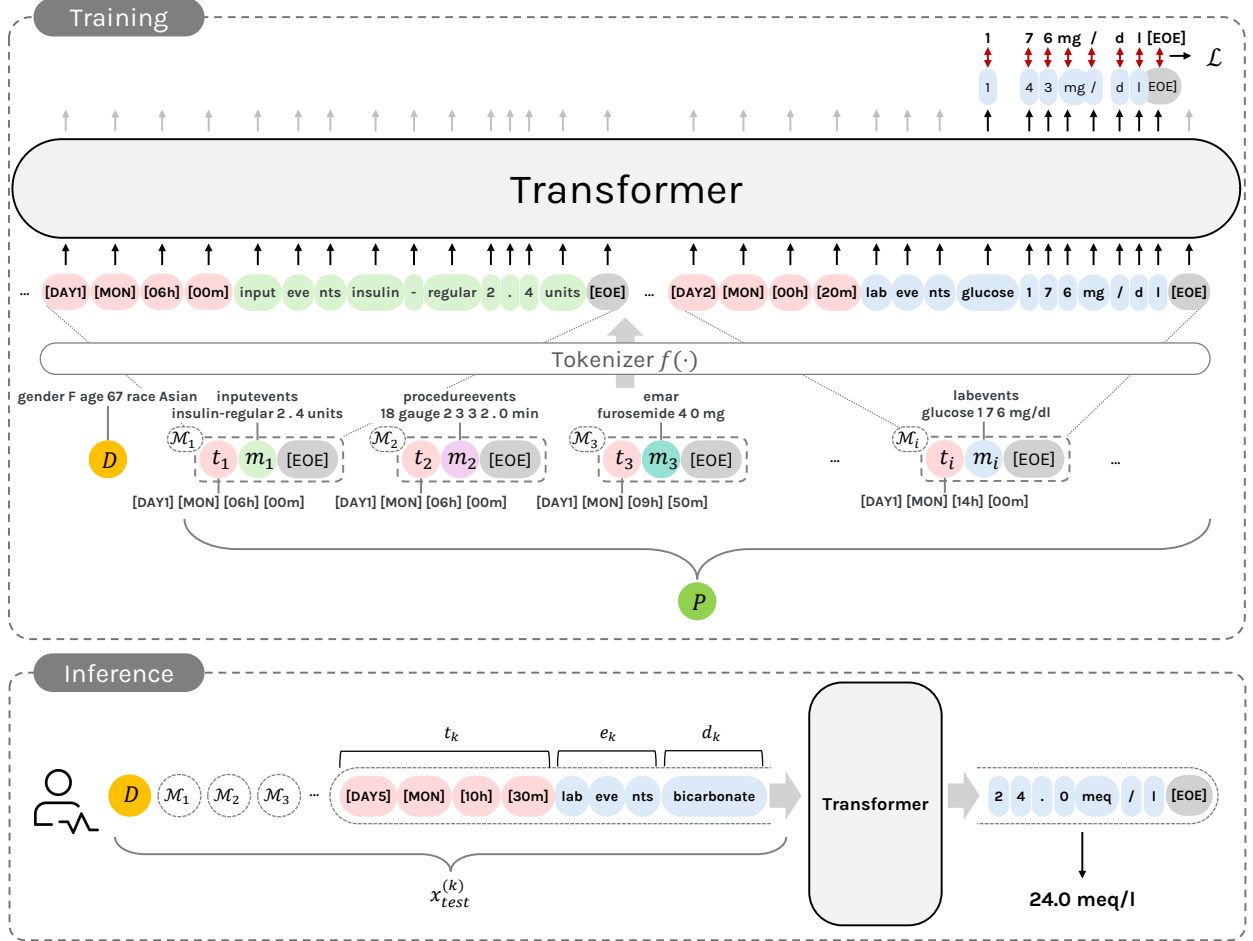


Figure 1: **Training and Inference of LabTOP.** During training, demographic information  $D$  and a sequence of medical events  $P = [\mathcal{M}_1, \dots, \mathcal{M}_N]$  are tokenized, and fed into the Transformer to generate next token at each position. The training loss is then computed only for lab test value tokens along with their units and the corresponding  $[EOE]$  token. During inference, given the preceding sequence of medical events and the target lab event (i.e.,  $(t_k, e_k, d_k)$ ), the model autoregressively generates numeric value tokens for its outcome until the  $[EOE]$  token is encountered.

ical code  $c_i$  into a fixed-dimensional vector space to represent a medical event  $\mathcal{M}_i$  (Miotto et al., 2016; Choi et al., 2016, 2020; Song et al., 2018; Shang et al., 2019; Renc et al., 2024), we start by converting each medical code  $c_i$  (e.g., “2160-0”) into its corresponding textual description  $d_i$  (e.g., “Creatinine [Mass/volume] in Serum or Plasma”). Additionally, we also treat its numerical value  $v_i$  as plain text and split it into each digit, so that each digit is processed as a separate token in the input sequence (Hur et al., 2022, 2023; Kim et al., 2023). In this way, we reconstruct a 4-subtuple of  $(e_i, c_i, v_i, u_i)$  included in the medical event  $\mathcal{M}_i$  into a textual sequence, and denote as  $m_i$ . For example, a lab test event standing

for a creatinine value of 1.23 mg/dL measured at the time of  $t_i$  is transformed into  $(t_i, m_i)$  where  $m_i$  is a plain text of “labevent creatinine 1 . 2 3 mg/dL”.

**Absolute time encoding** Temporal information also plays a crucial role in modeling the progression of a patient’s health status accurately, as the timing and frequency of the events provide essential insights into clinical trajectories. While previous studies have primarily employed a relative time encoding strategy to represent temporal intervals between consecutive events (Hur et al., 2023; Renc et al., 2024), this approach may not always be optimal due to the following reasons. Medical events for inpatients, such

as prescriptions and lab tests, usually follow regular patterns dictated by hospital routines, clinical protocols, or daily schedules. Additionally, a patient’s physiological status can also depend on time-of-day patterns, making absolute time representation more effective in capturing meaningful trends. For example, blood glucose measurements are heavily affected by a patient’s fasting state (Moebus et al., 2011). By incorporating absolute time encoding, the model can infer contextual factors such as feeding schedules or overnight fasting periods, leading to improved predictive performances for lab test outcomes.

To achieve this, we represent each timestamp  $t_i$  as a combination of four types of special tokens, capturing essential temporal attributes that influence patient health status. Specifically, these tokens include (1) the elapsed days since the ICU admission, (2) the day of the week the event occurred, (3) the absolute hour of the event, and (4) the aggregated minute value. The minute value is aggregated in 10-minute intervals to balance granularity and computational efficiency, ensuring that time representations remain meaningful without introducing excessive sparsity. For example, for the event recorded on the first day since the ICU admission, at 13:38 on a Tuesday, the timestamp  $t_i$  is defined as  $[\text{DAY1}], [\text{TUE}], [13\text{h}], [30\text{m}]]$ . In addition, we append a special  $[\text{EOE}]$  token indicating the end of the event to every textual medical event  $m_i$  and concatenate a sequence of medical events, so that a patient  $P$  is now represented as

$$P = \left\|_{i=1}^N [t_i, m_i, [\text{EOE}]] \right\| \quad (1)$$

where  $\|$  is a symbol denoting the sequence concatenation operator.

**Demographic encoding** Physiological ranges for lab tests can vary significantly based on demographic attributes such as age, gender, and race. For example, creatinine levels tend to be higher in males due to greater muscle mass (Culleton et al., 1999), while hemoglobin levels may vary depending on both gender and age (Murphy, 2014). To incorporate this information into our model, we convert each patient’s demographic attributes into a textual representation, denoted as  $D$ . For example, for a 65-year-old Asian female patient,  $D$  is defined as “gender F age 65 race Asian”. We prepend this demographic information to the patient’s sequence of medical events  $P$  and tokenize the sequence using the Bio-Clinical BERT tokenizer (Alsentzer et al., 2019) to obtain the final

input sequence for the model, which is defined as

$$x = f(D\|P) = f\left(\left\|_{i=1}^N [t_i, m_i, [\text{EOE}]]\right\|\right) \quad (2)$$

where  $f(\cdot)$  denotes the tokenization function that converts the text sequence into a sequence of token indices.

### 3.3. LabTOP Training

**Model architecture** We design our model following the GPT-2 architecture (Radford et al., 2019), which is composed of Transformer decoder layers (Vaswani, 2017). Specifically, the input sequence  $x$  is embedded into a sequence of latent vectors  $\mathbf{X} \in \mathbb{R}^{M \times h}$  by the learnable embedding layer, where  $M$  is the length of the input token sequence and  $h$  is the hidden dimension of the model. They are then fed into the Transformer decoder to model the conditional probability of the next token given the previous sequence, following an autoregressive language modeling approach.

**Objective** Unlike traditional language modeling where the objective is to predict the next token for every position in the sequence, we modify the loss computation to focus exclusively on lab test outcome prediction. That is, instead of computing the loss for all tokens, we selectively compute the loss only on the tokens corresponding to lab test values, encouraging the model to focus on accurately predicting lab test outcomes while still benefiting from a broader contextual understanding of the patient’s medical history. Accordingly, the loss is defined as

$$\mathcal{L} = - \sum_{i \in \mathcal{I}_{lab}} \log p(x_i | x_{<i}; \theta) \quad (3)$$

where  $\mathcal{I}_{lab}$  represents the set of token positions corresponding to lab test values along with their unit of measurements, as well as their special  $[\text{EOE}]$  token.

**Random permutation** As mentioned in the previous section, timestamps are discretized into 10-minute interval tokens (e.g., 13:38  $\rightarrow$   $[[13\text{h}], [30\text{m}]]$ ), which can result in multiple medical events having the same timestamp tokens. Accordingly, in order to make the model invariant to their ordering during training, we apply random permutation to medical events that share the same timestamp. Specifically, given a set of events having the same timestamp, we randomly shuffle the order of the events at each training iteration to prevent the model from overfitting to any arbitrary order within the same timestamp.

### 3.4. LabTOP Inference

We formulate the lab test outcome prediction task as a language modeling task to predict numeric values token-by-token in an autoregressive manner. That is, the model generates the corresponding numeric value of a target lab item given the sequence of prior medical events and the target lab item’s name. Accordingly, to construct inference samples, we extract every lab item appearing in the input sequence and build a corresponding inference prompt. Specifically, for each target lab test item occurring at timestamp  $t_k$ , we concatenate all prior medical events up to  $t_k$  along with the target lab test’s textual representation,  $e_k$  and  $d_k$ , to create an inference sequence. Thus, the  $k$ -th inference sample of a patient is defined as

$$x_{test}^{(k)} = f\left(D, \left\|_{t_i < t_k} [t_i, m_i, \text{[EOE]}], [t_k, e_k, d_k]\right\|\right) \quad (4)$$

where  $e_k$  and  $d_k$  denote the event type (*i.e.*, “labevent”) and textual description of the target lab test (*e.g.*, “bicarbonate”), as aforementioned.

Once the inference sequence is constructed, it is fed into the trained model, which generates tokens autoregressively until the [EOE] token is encountered. In this process, our primary objective is to accurately predict the outcome value of a specific lab test at a given timestamp rather than probabilistically generating potential future lab tests. Thus, to ensure precise predictions, we do not sample from the model’s output distribution but instead select the most probable token (*i.e.*, top-1 token) at each decoding step. The generated sequence is then decoded back into a numerical value (*e.g.*, 2 4 . 0 meq / l  $\rightarrow$  24.0 meq/l).

## 4. Experiments

### 4.1. Data

To demonstrate the generalizability of our approach, we conduct experiments on three publicly available EHR datasets: MIMIC-IV (Johnson et al., 2023), eICU (Pollard et al., 2018), and HiRID (Yèche et al., 2021). Specifically, MIMIC-IV consists of 94,458 ICU records of 364,627 patients from the Beth Israel Deaconess Medical Center, including structured time-series data such as lab test results, and medication administrations. eICU is a large-scale, multi-center dataset that includes 200,859 ICU records of 139,367 patients from hospitals across the United States, consisting of a broader range of patient demographics and treatment variations compared to single-center

datasets. HiRID is a high-resolution ICU dataset collected from the Bern University Hospital in Switzerland, composed of 33,905 ICU patients. For all these datasets, we take the ICU records whose length of stay is at least 6 hours. We then randomly split them into training, validation, and test sets in an 8:1:1 based on their patient IDs, and treat each ICU record as an individual sample for our model. Detailed dataset statistics are described in Appendix A.

To determine which types of EHR events should be involved for lab test outcome prediction, we categorized EHR events into two broad types: observation-type events, which represent the patient’s physiological state (*e.g.*, lab tests, microbiology tests), and intervention-type events, which correspond to medical treatments, prescriptions, and procedures administered during the ICU stay. We then prioritized these event types based on their expected influence on lab test results: (1) Firstly, medication events that directly reflect the patient’s physiological status by indicating administered drugs and dosages. (2) Secondly, other intervention-related events, including input events (*e.g.*, fluid intake) and procedure events, which affect the patient’s overall condition. (3) Lastly, observation-type events that do not directly alter a patient’s state but provide useful contextual information about their physiological trends. Based on these criteria, the following tables for each dataset are used:

- MIMIC-IV: *labevents*, *emar*, *emar\_detail*, *inputevents*, *procedureevents*, *outputevents*, *microbiologyevents*
- eICU: *lab*, *medication*, *infusiondrug*, *treatment*, *intakeoutput*, *microlab*
- HiRID: *observation\_tables*, *pharma\_records*

Note that HiRID collected every observation-type event into one table (*i.e.*, *observation\_tables*), which leads to multiple types of events, such as lab tests and microbiology tests, being contained in this single table. However, there is only an indicator specifying whether an event corresponds to a lab test or not, so we cannot differentiate other observation-type events within this table. Accordingly, we select only those events explicitly identified as lab tests, excluding all other events from this table.

Additionally, to ensure a focus on the most clinically relevant medical events, we select only the medical items that account for the top 90% of occurrences within their respective tables for each dataset,

including the lab test tables as well as other event types such as medication, input events, and procedure events. As a result, we select 44 unique lab tests from MIMIC-IV, 41 from eICU, and 27 from HiRID. The included lab items from each dataset are detailed in Appendix A.

#### 4.2. Evaluation Metrics

**NMAE** Normalized Mean Absolute Error (NMAE) is a normalized version of Mean Absolute Error (MAE) that accounts for differences in scale across multiple variables with different units and ranges. Unlike standard MAE, which directly measures the average absolute difference between the predicted and ground-truth values, NMAE adjusts for variations in measurement scales by normalizing each error term based on the range of the corresponding lab item. Specifically, for each unique lab item  $l$ , we compute its scale using the difference between the 99th percentile and the 1st percentile values (*i.e.*,  $v_{99\%}^{(l)} - v_{1\%}^{(l)}$ ) in the test set to mitigate the influence of extreme outliers. The NMAE for a given lab test  $l$  is then computed by dividing its MAE by this scale, which is defined as

$$\text{NMAE}_l = \frac{1}{v_{99\%}^{(l)} - v_{1\%}^{(l)}} \sum_{i \in \mathcal{I}_l} \frac{|y_i - \hat{y}_i|}{N_l} \quad (5)$$

where  $\mathcal{I}_l$  represents the set of sample indices corresponding to the target lab test,  $y_i$  and  $\hat{y}_i$  denote the ground-truth and predicted value for  $i$ -th sample, and  $N_l$  is the number of target lab samples in the test set.

**SMAPE** Symmetric Mean Absolute Percentage Error (SMAPE) is a widely used metric to evaluate the accuracy of prediction for continuous values, providing an intuitive measure of how much predicted values deviate from ground-truth values in percentage terms. Unlike traditional Mean Absolute Percentage Error (MAPE), SMAPE ensures a symmetric scaling by normalizing the error terms based on the sum of the absolute values of the ground-truth and predicted values, preventing over-penalization when the ground-truth values are small. This property makes SMAPE especially suitable for evaluating lab test outcome predictions, where the ranges of different lab items can vary significantly. The SMAPE for a given lab test  $l$  is defined as

$$\text{SMAPE}_l = \frac{1}{N_l} \sum_{i \in \mathcal{I}_l} \frac{|y_i - \hat{y}_i|}{(|y_i| + |\hat{y}_i|)/2} \times 100 \quad (6)$$

#### 4.3. Baselines

To demonstrate the effectiveness of LabTOP, we compare its performance with the following baseline methods, including both traditional machine learning approaches and state-of-the-art LLMs.

- **Naive:** A simple method that predicts the lab test value at a given timestamp by using the most recent measured value of the same lab test, commonly referred to as the naive forecasting method.
- **Naive( $\mu$ ):** A variant of the naive method that predicts the lab test value by averaging all previously recorded values of the same lab test before the prediction timestamp.
- **GenHPF (Hur et al., 2023):** A multi-task learning model that incorporates hierarchical patient features for clinical prediction tasks. We adapt GenHPF to estimate lab test values by formulating it as a regression task.
- **XGBoost (Chen and Guestrin, 2016):** A widely used gradient boosting method designed for structured data. For this baseline, we use several statistics of past measurements, such as count and mean.
- **GPT-4o and GPT-4o-mini:** LLMs designed for general-purpose tasks. We evaluate these models to assess the capability of general-purpose models in predicting lab test outcomes. Since these models process long patient histories as input, running inference across the entire test set would require substantial token usage. To balance computational feasibility with representative evaluation, we sample 10% of the test set<sup>2</sup>. All experiments employing GPTs were executed using the HIPAA-compliant GPT model available on Azure.<sup>3</sup>
- **LLaMA-3.1-Instruct (8B) (Grattafiori et al., 2024):** We also evaluate the open-sourced instruction-tuned LLM designed for general-purpose tasks. For the experiments on this large model, we sample 10% of the test set as the same with GPT-4o and GPT-4o-mini.

2. To be more specific, running inference in a batch on the sampled 10% of the test set incurred a total cost of approximately \$500.

3. <https://learn.microsoft.com/en-us/azure/compliance/offerings/offering-hipaa-us>

Table 1: Lab test outcome prediction performances on different EHR datasets, where mean and 95% confidence interval are shown across 3 different random seeds for trainable models (e.g., GenHPF, XGBoost, and LabTOP). The best performances for each dataset are highlighted with **boldface**.

	MIMIC-IV	eICU	HiRID
<b>NMAE</b>			
Naive	0.090	0.102	0.101
Naive( $\mu$ )	0.108	0.116	0.119
GenHPF	0.112 $\pm$ 0.007	0.106 $\pm$ 0.011	0.127 $\pm$ 0.027
XGBoost	0.083 $\pm$ 0.000	0.475 $\pm$ 0.000	0.100 $\pm$ 0.000
GPT-4o	0.195	0.230	0.165
GPT-4o-mini	0.792	1.027	2.969
LLaMA-3.1-Inst.	1.271	1.570	3.280
<b>LabTOP</b>	<b>0.064<math>\pm</math>0.001</b>	<b>0.080<math>\pm</math>0.007</b>	<b>0.083<math>\pm</math>0.004</b>
<b>SMAPE (%)</b>			
Naive	17.64	18.29	<b>15.98</b>
Naive( $\mu$ )	21.78	20.83	18.99
GenHPF	25.58 $\pm$ 0.52	24.22 $\pm$ 1.30	19.18 $\pm$ 2.98
XGBoost	20.42 $\pm$ 0.00	45.86 $\pm$ 0.00	17.18 $\pm$ 0.00
GPT-4o	19.67	21.18	21.17
GPT-4o-mini	40.86	45.67	43.88
LLaMA-3.1-Inst.	75.58	79.92	76.63
<b>LabTOP</b>	<b>14.80<math>\pm</math>0.13</b>	<b>15.96<math>\pm</math>0.22</b>	16.83 $\pm$ 0.21

More details about each model’s implementation, such as training hyperparameters and feature engineering for XGBoost, are provided in Appendix B.

#### 4.4. Results

The average results of lab test outcome prediction for three datasets are presented in Table 1.

LabTOP achieves the best performance in both NMAE and SMAPE across all datasets, except for NMAE in HiRID, where it still performs competitively. Notably, naive approaches (Naive and Naive( $\mu$ )) show relatively higher SMAPE in HiRID compared to MIMIC-IV and eICU. We speculate that this is due to the characteristics of HiRID, where lab tests are conducted more frequently than in the other two datasets. Specifically, we found that the average interval between lab measurements is about 15.8 hours in MIMIC-IV, 19.8 hours in eICU, and only 12.9 hours in HiRID. This shorter interval likely benefits methods that rely on simple statistical heuristics, such as carrying forward the last measured value (Naive) or computing historical averages (Naive( $\mu$ )), making them more effective in this setting. However, our primary motivation is to predict lab test

outcomes in environments where frequent testing is not always feasible. Given this perspective, the strong performance of LabTOP on MIMIC-IV and eICU highlights its effectiveness in scenarios where repeated testing may not be feasible.

Interestingly, LabTOP also outperforms general-purpose LLMs (GPT-4o, GPT-4o-mini, and LLaMA-3.1-Instruct), confirming that these models struggle with lab test outcome prediction task. This underscores the importance of explicitly learning EHR data rather than relying on general LLM capabilities. Furthermore, GPT-4o-mini and LLaMA-3.1-Instruct exhibit significantly lower performance, which we attribute to its tendency to generate unrealistic lab test values. Upon manual inspection, we found that GPT-4o-mini and LLaMA-3.1-Instruct often output numerically implausible values that are far outside the expected range (e.g., predicting *ph of arterial blood* as 135 whereas the ground-truth is 7.2). This result demonstrates that our data processing and training strategy play a crucial role in achieving robust performance by effectively leading the model to produce clinically meaningful predictions.

#### 4.5. Ablation Studies

To systematically evaluate the contributions of different components in our model, we conduct ablation studies along the following perspectives. All experiments in this section are conducted using the MIMIC-IV dataset to ensure consistency.

##### 4.5.1. EMBEDDING AND TRAINING STRATEGY

EHR events can be processed using different embedding strategies, which we categorize into **code-based** and **text-based** representations. The code-based approach directly embeds structured medical codes (e.g., LOINC, ICD), while the text-based approach converts medical codes into their textual descriptions before embedding. Additionally, unlike conventional methods that apply autoregressive loss to all tokens (i.e., **Full AR**), we specifically designed our model to focus on lab test values by applying autoregressive loss selectively (i.e., **Only LAB AR**). To examine the impact of these design choices, we compare our model trained with different combinations of embeddings and loss strategies.

In the code-based embedding strategy, a new vocabulary is defined to accommodate structured medical tokens, following the embedding approach introduced in ETHOS (Renc et al., 2024). Specifically,

Table 2: Ablation study results from different perspectives on MIMIC-IV dataset.

Strategy	NMAE	SMAPE (%)
<i>Embedding &amp; training strategy</i>		
code-based & Full AR	0.106 $\pm$ 0.005	20.97 $\pm$ 0.33
code-based & Only Lab AR	0.098 $\pm$ 0.002	19.44 $\pm$ 0.55
text-based & Only Lab AR ( <b>LabTOP</b> )	<b>0.064<math>\pm</math>0.001</b>	<b>14.80<math>\pm</math>0.13</b>
<i>Numeric value representation</i>		
5-quantiles	0.077 $\pm$ 0.001	18.27 $\pm$ 0.11
quantile-based 10-quantiles	0.072 $\pm$ 0.000	16.64 $\pm$ 0.14
20-quantiles	0.067 $\pm$ 0.001	15.65 $\pm$ 0.01
digit-wise tokenization ( <b>LabTOP</b> )	<b>0.064<math>\pm</math>0.001</b>	<b>14.80<math>\pm</math>0.13</b>
<i>Timestamp representation</i>		
relative time encoding	0.134 $\pm$ 0.001	29.02 $\pm$ 0.05
absolute time encoding ( <b>LabTOP</b> )	<b>0.064<math>\pm</math>0.001</b>	<b>14.80<math>\pm</math>0.13</b>

one or two tokens are defined per event: one token for the total event features that encodes the event type, item name and unit of measurement (if applicable) as a single entity (*e.g.*, [LAB\_inr(pt)] or [LAB\_glucose\_mg/dL]), and the other token for the corresponding value mapped to one of 10 quantile tokens if the event has a numeric value. Additionally, for medications, we map drug names to their corresponding ATC (Anatomical Therapeutic Chemical) codes whenever available.

As shown in Table 2, the incremental application of our embedding and training strategy components consistently improves performance. Specifically, switching from training all tokens in an autoregressive manner to focusing solely on lab test events has a positive impact on the model’s predictive accuracy. This suggests that selective loss computation allows the model to effectively develop a deeper understanding of patterns and relationships specific to lab test outcomes. In addition, incorporating a text-based embedding approach further enhances performance. This improvement again highlights the advantage of providing the model with rich and interpretable representations of medical events, enabling it to better capture relationships within EHR data.

#### 4.5.2. NUMERIC VALUE REPRESENTATION

An alternative approach to handling numeric values in language models is discretization into quantiles,

where continuous values are mapped to a set of pre-defined bins and treated as categorical tokens (*i.e.*, **quantile-based tokenization**) (Renc et al., 2024). In contrast, our model treats numeric values as text and tokenizes them at the digit level (*i.e.*, **digit-wise tokenization**). To evaluate the effectiveness of this approach against the quantile-based method, we conduct experiments using different levels of quantization (5, 10, and 20 quantiles) and compare the results with the digit-wise tokenization strategy.

For the quantile-based method, the predicted value  $\hat{y}$  is computed as the expected value of the quantile probabilities for each lab item. Specifically, given a set of quantile bins  $\mathcal{Q}$ , each bin  $q \in \mathcal{Q}$  is associated with a probability  $p(q)$ . The predicted value is defined as the weighted sum of the expected values of the quantile intervals:

$$\hat{y} = \sum_{q \in \mathcal{Q}} \mu_q \cdot p(q) \quad (7)$$

where  $\mu_q$  is the average value of the target lab item samples belonging to the quantile  $q$  in the training set.

As shown in Table 2, performance improves consistently as the number of quantile bins increases, suggesting that finer-grained numeric representations lead to better predictions. Following this trend, digit-wise tokenization, as used in LabTOP, achieves the best performance, likely because it provides the highest resolution representation by preserving the exact numerical value rather than grouping them into fixed bins. We believe this approach allows the model to capture subtle variations in lab test values that might otherwise be lost in a coarser representation. Thus, these results highlight the importance of maintaining fine-grained detail when encoding numerical values to process EHR data effectively.

#### 4.5.3. TIMESTAMP REPRESENTATION

As discussed in Section 3.2, a patient’s medical state can be influenced by daily routines and hospital schedules, making absolute time encoding more suitable than relative time encoding. To validate the effectiveness of our approach, we compare our model trained with **relative time encoding** against the one trained with **absolute time encoding**, as presented in Table 2. For relative time encoding, we calculate temporal intervals in minutes between consecutive events and append each interval to the corresponding medical event  $\mathcal{M}_i$  after converting it to

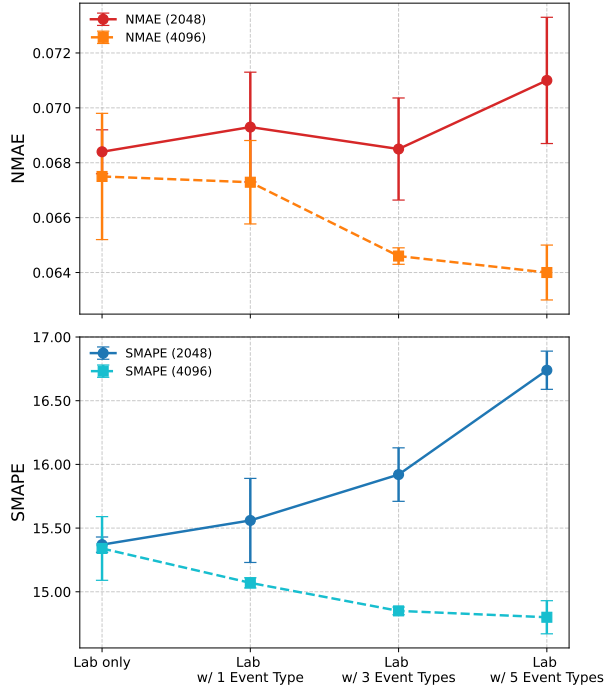


Figure 2: Performance trends across different configurations of event types.

a text format, instead of prepending absolute timestamp tokens which we defined.

The result demonstrates that absolute time encoding leads to superior performance compared to relative time encoding, suggesting that absolute time encoding implicitly provides a more meaningful temporal context than merely representing time as intervals between events. In other words, absolute time encoding allows the model to capture daily patterns and periodic trends that influence lab test results, such as fasting-related fluctuations in glucose levels or routine morning lab draws in ICU settings. In contrast, relative time encoding only provides information about the time elapsed since the previous event, making it more challenging for the model to infer broader temporal structures. These findings emphasize the importance of designing time representations that align with the structured nature of clinical workflows.

#### 4.5.4. COMBINATION OF DIFFERENT EVENT TYPES

As described in Section 4.1, we prioritized event types into three levels based on their expected influence on lab test results. To assess how including a broader

range of clinical events affects performances, we train models with different configurations of event types according to the criterion described in Section 4.1, and analyze their performance trends. Specifically, each configuration incrementally includes (1) medication events (*i.e.*, *emar* and *emar\_detail*), (2) input and procedure events (*i.e.*, *inputevents* and *procedureevents*), and (3) output and microbiology events (*i.e.*, *outputevents* and *microbiologyevents*). Here, while utilizing more event types can provide richer contextual information, it can also lead the model to see a shorter historical window within the fixed sequence length. For example, when using only two types of events (lab test and medication), the average covered time span per sample is 28.8 hours with a sequence length of 2048 tokens and 47.2 hours with 4096 tokens. In contrast, when including six types of events, the average covered time span drops to 18.5 hours for 2048 tokens and 33.3 hours for 4096 tokens. Hence, to systematically examine this trade-off, we also conduct these experiments by adjusting the sequence length to 2048 tokens from 4096 tokens, and compare the trends between them. Detailed statistics on the average covered time span for each table combination are provided in Appendix A.

Figure 2 illustrates the impact of progressively incorporating more event types on the lab test outcome prediction performances. The results show that when the sequence length is limited to 2048 tokens, increasing the number of event types leads to a degradation in performance for both sMAE and SMAPE. This suggests that the reduced temporal coverage outweighs the benefits of incorporating more event types in this constrained setting. In contrast, when using a sequence length of 4096 tokens, expanding the range of event types improves performance in general, indicating that longer sequences allow the model to leverage additional event information effectively. These findings suggest that while our current experiments are still constrained to a sequence length of 4096 tokens, further increasing the sequence length may unlock additional benefits from incorporating an even broader range of EHR event types.

## 5. Conclusion and Discussion

In this work, we proposed **LabTOP**, a unified model for lab test outcome prediction that leverages an autoregressive generative modeling approach on EHR data. By integrating effective data processing and training strategy, LabTOP has shown the best per-

formance across three public EHR datasets. Specifically, through evaluations on MIMIC-IV, eICU, and HiRID, LabTOP consistently outperformed both traditional machine learning models and state-of-the-art LLMs, demonstrating its potential for clinical decision support and early detection of critical conditions. Additionally, our ablation studies highlighted the efficacy of the proposed data processing and training strategy in modeling EHR data for the lab test outcome prediction task. We believe that LabTOP will serve as an accurate and generalizable framework for lab test outcome prediction, especially in constrained environments where repeated testing is not feasible.

**Clinical utility of LabTOP** Our model allows for the quantification of uncertainty in its predictions, which can be measured using the average entropy of token probabilities when generating lab test values. For example, if a model outputs “1 2 3 . 4 5”, we can compute entropies for the generated tokens (“1”, “2”, “3”, “.”, “4”, and “5”) and average them to get the uncertainty of the predicted output. By leveraging this uncertainty estimation, high-confidence predictions can be directly used for clinical decision support, while low-confidence predictions can be flagged for further verification through actual lab testing. This approach helps prioritize critical tests while reducing unnecessary routine tests. As a specific scenario, in ICUs and other hospital settings where continuous monitoring is critical, patients frequently undergo multiple daily lab tests to assess their condition. However, frequent blood draws can lead to increased risk of anemia and additional workload for healthcare providers. According to [James et al. \(2018\)](#), ICU patients often undergo 1-4 blood tests per day, and repeated phlebotomy is a major contributor to anemia in critically ill patients. In this scenario, by incorporating LabTOP into clinical workflows, healthcare providers could pre-screen lab test predictions and selectively order confirmatory tests only when predictions exhibit high uncertainty. This approach would reduce unnecessary testing, helping to minimize patient burden and optimize resource allocation while maintaining diagnostic accuracy.

**Limitations and future work** Our experiments have some limitations as follows. First, LabTOP requires relatively longer sequence length, leading to increased computational costs during training and inference, especially when we involve more types of EHR events. To mitigate this, we applied optimiza-

tion techniques such as mixed-precision training to enhance GPU memory efficiency. Despite these optimizations, memory usage and inference latency remain key concerns for real-world deployment. Future work could explore more efficient tokenization strategies to balance precision and computational efficiency. Second, our experiments were focused on retrospective EHR data, and its real-world applicability in prospective clinical settings remains to be validated. Further research could assess LabTOP’s performance in real-time hospital environments and evaluate its impact on clinical decision-making. Finally, generalization beyond ICU settings needs further investigation. Our current model is designed for short-term (near-future) prediction, leveraging high-density time-series data and trained in an autoregressive manner. This setup aligns well with ICU and inpatient settings, where lab tests are recorded at high frequency and recent trends play a crucial role in clinical decision-making. In contrast, medical records for the general population tend to be recorded at irregular intervals, often spanning months or years between visits. Under such conditions, our training and inference strategy may not generalize effectively. Instead of directly applying LabTOP in this setting, a more suitable approach may involve alternative modeling techniques, such as point process-based models or learning strategies specifically designed for sparse and irregular medical data, which would be an interesting future research direction.

## Acknowledgments

This work was supported by the Institute of Information & Communications Technology Planning & Evaluation (IITP) grant (No.RS-2019-II190075), National Research Foundation of Korea (NRF) grant (NRF-2020H1D3A2A03100945, RS-2023-00262527), funded by the Korea government (MSIT).

## References

- Emily Alsentzer, John R Murphy, Willie Boag, Wei-Hung Weng, Di Jin, Tristan Naumann, and Matthew McDermott. Publicly available clinical bert embeddings. *arXiv preprint arXiv:1904.03323*, 2019.
- Anshula Ambasta, Stefana Pancic, Brian M Wong, Todd Lee, Deirdre McCaughey, and Irene WY Ma. Expert recommendations on frequency of utilization of common laboratory tests in medical inpatients: a canadian consensus study. *Journal of General Internal Medicine*, 34:2786–2795, 2019.
- Imelda Cabalar, Thu H Le, Abigail Silber, Matthew O’Hara, Bilal Abdallah, Monisha Parikh, and Robert Busch. The role of blood testing in prevention, diagnosis, and management of chronic diseases: A review. *The American Journal of the Medical Sciences*, 2024.
- Tianqi Chen and Carlos Guestrin. Xgboost: A scalable tree boosting system. In *Proceedings of the 22nd acm sigkdd international conference on knowledge discovery and data mining*, pages 785–794, 2016.
- Edward Choi, Mohammad Taha Bahadori, Andy Schuetz, Walter F Stewart, and Jimeng Sun. Doctor ai: Predicting clinical events via recurrent neural networks. In *Machine learning for healthcare conference*, pages 301–318. PMLR, 2016.
- Edward Choi, Zhen Xu, Yujia Li, Michael Dusenberry, Gerardo Flores, Emily Xue, and Andrew Dai. Learning the graphical structure of electronic health records with graph convolutional transformer. In *Proceedings of the AAAI conference on artificial intelligence*, volume 34, pages 606–613, 2020.
- Bruce F Culleton, Martin G Larson, Jane C Evans, Peter WF Wilson, Brendan J Barrett, Patrick S Parfrey, and Daniel Levy. Prevalence and correlates of elevated serum creatinine levels: the framingham heart study. *Archives of internal medicine*, 159(15):1785–1790, 1999.
- Tony Duan, Avati Anand, Daisy Yi Ding, Khanh K Thai, Sanjay Basu, Andrew Ng, and Alejandro Schuler. Ngboost: Natural gradient boosting for probabilistic prediction. In *International conference on machine learning*, pages 2690–2700. PMLR, 2020.
- Martin Faltys, Marc Zimmermann, Xinrui Lyu, Matthias Hüser, Stephanie L Hyland, Gunnar Rätsch, and Tobias Merz. Hirid, a high time-resolution icu dataset (version 1.1.1), 2021.
- Xiaomin Fu, Yuhan Wang, Ryan S Cates, Nan Li, Jing Liu, Dianshan Ke, Jinghua Liu, Hongzhou Liu, and Shuangtong Yan. Implementation of five machine learning methods to predict the 52-week blood glucose level in patients with type 2 diabetes. *Frontiers in Endocrinology*, 13:1061507, 2023.
- Aaron Grattafiori, Abhimanyu Dubey, Abhinav Jauhri, Abhinav Pandey, Abhishek Kadian, Ahmad Al-Dahle, Aiesha Letman, Akhil Mathur, Alan Schelten, Alex Vaughan, et al. The llama 3 herd of models. *arXiv preprint arXiv:2407.21783*, 2024.
- Tracy D Gunter and Nicolas P Terry. The emergence of national electronic health record architectures in the united states and australia: models, costs, and questions. *Journal of medical Internet research*, 7(1):e383, 2005.
- Kyunghoon Hur, Jiyoung Lee, Jungwoo Oh, Wesley Price, Younghak Kim, and Edward Choi. Unifying heterogeneous electronic health records systems via text-based code embedding. In *Conference on Health, Inference, and Learning*, pages 183–203. PMLR, 2022.
- Kyunghoon Hur, Jungwoo Oh, Junu Kim, Jiyoun Kim, Min Jae Lee, Eunbyeol Cho, Seong-Eun Moon, Young-Hak Kim, Louis Atallah, and Edward Choi. Genhpf: General healthcare predictive framework for multi-task multi-source learning. *IEEE Journal of Biomedical and Health Informatics*, 2023.
- Stephanie L Hyland, Martin Faltys, Matthias Hüser, Xinrui Lyu, Thomas Gumbsch, Cristóbal Esteban, Christian Bock, Max Horn, Michael Moor, Bastian Rieck, et al. Early prediction of circulatory failure in the intensive care unit using machine learning. *Nature medicine*, 26(3):364–373, 2020.
- Tyler Edward James, Rebecca Barty, Yang Liu, Bram Rochweg, Nancy Heddle, and Deborah M Siegal. Blood loss due to laboratory testing in critical care patients: a retrospective cohort study. *Blood*, 132:4885, 2018.

- Yixing Jiang, Andrew H Lee, Xiaoyuan Ni, Conor K Corbin, Jeremy A Irvin, Andrew Y Ng, and Jonathan H Chen. Probabilistic prediction of laboratory test information yield. In *AMIA Annual Symposium Proceedings*, volume 2023, page 1007, 2024.
- Alistair Johnson, Lucas Bulgarelli, Tom Pollard, Steven Horng, Leo Anthony Celi, and Roger Mark. Mimic-iv (version 3.1), 2020.
- Alistair EW Johnson, Lucas Bulgarelli, Lu Shen, Alvin Gayles, Ayad Shammout, Steven Horng, Tom J Pollard, Sicheng Hao, Benjamin Moody, Brian Gow, et al. Mimic-iv, a freely accessible electronic health record dataset. *Scientific data*, 10(1):1, 2023.
- Junu Kim, Chaeun Shim, Bosco Seong Kyu Yang, Chami Im, Sung Yoon Lim, Han-Gil Jeong, and Edward Choi. General-purpose retrieval-enhanced medical prediction model using near-infinite history. *arXiv preprint arXiv:2310.20204*, 2023.
- Zeljko Kraljevic, Anthony Shek, Daniel Bean, Rebecca Bendayan, James Teo, and Richard Dobson. Medgpt: Medical concept prediction from clinical narratives. *arXiv preprint arXiv:2107.03134*, 2021.
- Clemens Scott Kruse, Michael Mileski, Alekhya Ganta Vijaykumar, Sneha Vishnampet Viswanathan, Ujwala Suskandla, and Yazhini Chidambaram. Impact of electronic health records on long-term care facilities: systematic review. *JMIR medical informatics*, 5(3):e7958, 2017.
- Saúl Langarica, Diego de la Vega, Nawel Cariman, Martín Miranda, David C Andrade, Felipe Núñez, and Maria Rodriguez-Fernandez. Deep learning-based glucose prediction models: A guide for practitioners and a curated dataset for improved diabetes management. *IEEE Open Journal of Engineering in Medicine and Biology*, 2024.
- Kui Liu, Linyi Li, Yifei Ma, Jun Jiang, Zhenhua Liu, Zichen Ye, Shuang Liu, Chen Pu, Changsheng Chen, Yi Wan, et al. Machine learning models for blood glucose level prediction in patients with diabetes mellitus: Systematic review and network meta-analysis. *JMIR Medical Informatics*, 11(1):e47833, 2023.
- Riccardo Miotto, Li Li, Brian A Kidd, and Joel T Dudley. Deep patient: an unsupervised representation to predict the future of patients from the electronic health records. *Scientific reports*, 6(1):1–10, 2016.
- Susanne Moebus, Laura Göres, Christian Lösch, and Karl-Heinz Jöckel. Impact of time since last caloric intake on blood glucose levels. *European journal of epidemiology*, 26:719–728, 2011.
- William G Murphy. The sex difference in haemoglobin levels in adults—mechanisms, causes, and consequences. *Blood reviews*, 28(2):41–47, 2014.
- Tom J Pollard, Alistair EW Johnson, Jesse D Raffa, Leo A Celi, Roger G Mark, and Omar Badawi. The eicu collaborative research database, a freely available multi-center database for critical care research. *Scientific data*, 5(1):1–13, 2018.
- Tom J Pollard, Alistair EW Johnson, Jesse D Raffa, Leo A Celi, Roger G Mark, and Omar Badawi. eicu collaborative research database (version 2.0), 2019.
- Alec Radford, Karthik Narasimhan, Tim Salimans, and Ilya Sutskever. Improving language understanding by generative pre-training. 2018.
- Alec Radford, Jeffrey Wu, Rewon Child, David Luan, Dario Amodei, Ilya Sutskever, et al. Language models are unsupervised multitask learners. *OpenAI blog*, 1(8):9, 2019.
- Pawel Renc, Yugang Jia, Anthony E Samir, Jaroslaw Was, Quanzheng Li, David W Bates, and Arkadiusz Sitek. Zero shot health trajectory prediction using transformer. *NPJ Digital Medicine*, 7(1):256, 2024.
- Yulia Rubanova, Ricky TQ Chen, and David K Duvenaud. Latent ordinary differential equations for irregularly-sampled time series. *Advances in neural information processing systems*, 32, 2019.
- Mona Schirmer, Mazin Eltayeb, Stefan Lessmann, and Maja Rudolph. Modeling irregular time series with continuous recurrent units. In *International conference on machine learning*, pages 19388–19405. PMLR, 2022.
- Junyuan Shang, Tengfei Ma, Cao Xiao, and Jimeng Sun. Pre-training of graph augmented transformers for medication recommendation. *arXiv preprint arXiv:1906.00346*, 2019.

- Melashu Balew Shiferaw and Gizachew Yismaw. Magnitude of delayed turnaround time of laboratory results in amhara public health institute, bahir dar, ethiopia. *BMC health services research*, 19:1–6, 2019.
- Kenneth A Sikaris. Enhancing the clinical value of medical laboratory testing. *The Clinical Biochemist Reviews*, 38(3):107, 2017.
- Huan Song, Deepta Rajan, Jayaraman Thiagarajan, and Andreas Spanias. Attend and diagnose: Clinical time series analysis using attention models. In *Proceedings of the AAAI conference on artificial intelligence*, volume 32, 2018.
- A Vaswani. Attention is all you need. *Advances in Neural Information Processing Systems*, 2017.
- Michael Wornow, Rahul Thapa, Ethan Steinberg, Jason Fries, and Nigam Shah. Ehrshot: An ehr benchmark for few-shot evaluation of foundation models. *Advances in Neural Information Processing Systems*, 36:67125–67137, 2023.
- Cao Xiao, Tengfei Ma, Adji B Dieng, David M Blei, and Fei Wang. Readmission prediction via deep contextual embedding of clinical concepts. *PloS one*, 13(4):e0195024, 2018.
- Hugo Yèche, Rita Kuznetsova, Marc Zimmermann, Matthias Hüser, Xinrui Lyu, Martin Faltys, and Gunnar Rätsch. Hirid-icu-benchmark—a comprehensive machine learning benchmark on high-resolution icu data. *arXiv preprint arXiv:2111.08536*, 2021.
- Zhuo Zhi, Moe Elbadawi, Adam Daneshmend, Mine Orlu, Abdul Basit, Andreas Demosthenous, and Miguel Rodrigues. Hgbnet: predicting hemoglobin level/anemia degree from ehr data. *arXiv preprint arXiv:2401.12002*, 2024.

## Appendix A. Dataset Statistics

In this appendix, we describe dataset statistics used throughout our experiments.

Table 3: Number of ICU stays in the training, validation, and test splits for each dataset (MIMIC-IV, eICU, and HiRID).

	MIMIC-IV	eICU	HiRID
Train	73,236	141,712	26,597
Validation	9,151	17,716	3,325
Test	9,152	17,710	3,323

**Number of ICU records** Table 3 presents the number of ICU records in the training, validation, and test splits for each dataset (MIMIC-IV, eICU, and HiRID). We split ICU records based on a patient level, ensuring that records from the same patient do not appear in multiple subsets. The datasets follow an 8:1:1 split ratio, where 80% of ICU records are assigned to training, 10% to validation, and 10% to test splits.

Table 4: Number of lab events in the training, validation, and test splits for each dataset.

	MIMIC-IV	eICU	HiRID
Train	14,716,753	15,225,218	3,768,827
Validation	1,739,599	1,914,090	454,994
Test	1,799,223	1,848,832	456,609

**Number of lab test events** Table 4 presents the number of lab test events that appeared in the training, validation, and test splits for each dataset. Given the substantial volume of data, the model was exposed to a diverse range of lab test events, enabling a thorough evaluation of its ability to predict lab test outcomes.

**Selected lab items** To focus on the most clinically relevant medical events, we selected lab tests and other event types based on their frequency, retaining only those that accounted for the top 90% occurrences within their respective tables. As a result, we

Table 5: Average time span per sample in hours on MIMIC-IV.

Sequence Length	Lab-only	Lab w/ T1	Lab w/ T2	Lab w/ T3
2048	32.8	20.0	20.5	18.5
4096	43.6	34.8	23.1	20.3

T1: {medication event}

T2: T1  $\cup$  {input and procedure events}

T3: T2  $\cup$  {output and microbiology events}

included 44 lab tests from MIMIC-IV, 41 from eICU, and 27 from HiRID, as shown in Table 6. While core biomarkers such as glucose, sodium, potassium, chloride, creatinine, bicarbonate, hemoglobin, platelets, and white blood cell count are present across all datasets, notable differences exist: (1) MIMIC-IV includes a broader set of liver function tests (AST, ALT, bilirubin), coagulation markers (PT, INR), and red blood cell indices (MCV, MCH, RDW); (2) eICU incorporates hematological parameters (MPV, lymphocytes, monocytes) and oxygenation measures (FiO2, O2 saturation, base excess); and (3) HiRID focuses more on arterial blood gas (ABG) parameters (pH, PaO2, PaCO2, lactate, methemoglobin, carboxyhemoglobin), reflecting its emphasis on real-time ICU monitoring.

**Time span coverage per sample** Table 5 presents the average time span per sample (in hours) for different combinations of event types in MIMIC-IV, according to a sequence length of 2048 and 4096 tokens. The time span represents the total duration covered within each sample’s sequence. As expected, increasing the sequence length from 2048 to 4096 results in a longer time span coverage across all event combinations. Specifically, for lab-only sequences, the time span increases from 32.8 hours to 43.6 hours. However, adding more event types reduces the time span per sample, as additional events make each sample more dense within the same sequence length. For example, when we use a sequence length of 2048 tokens, incorporating one event type (Lab w/ T1) reduces the time span to 20.0 hours, while including two and four more event types (Lab w/ T2 and Lab w/ T3) results in 20.5 hours and 18.5 hours respectively. Similarly, for a sequence length of 4096 tokens, the time span decreases from 43.6 hours (Lab-only)

to 34.8 hours (Lab w/ T1), 23.1 hours (Lab w/ T2), and 20.3 hours (Lab w/ T3).

**Time intervals for each lab item** Tables 7, 8 and 9 present the time granularity (in hours) of lab items in MIMIC-IV, eICU, and HiRID, respectively. The time interval for each lab item represents the average interval (in hours) at which the lab item was recorded. A comparison of these tables reveals that the intervals between the same lab items are shortest in HiRID, indicating that lab tests are conducted more frequently in HiRID than in the other datasets.

## Appendix B. Implementation Details

This appendix provides implementation details, including data processing methods, model configurations, training hyperparameters, data processing steps, and hardware specifications used in the experiments.

**LabTOP** The model architecture of LabTOP follows GPT-2, specifically implemented using the architecture of HuggingFace GPT2LMHeadModel<sup>4</sup>. We use 12 attention decoder layers, each with 8 heads and a hidden dimension of 512. All the experiments in this study are conducted using a maximum sequence length of 4096 tokens by default. If a sequence of an ICU record exceeds the maximum sequence length, we repeatedly crop the sequence by this maximum length based on the event level. Additionally, we again prepend demographic information  $D$  to all the cropped samples. For training, we applied early stopping with the patience of 5 epochs based on the validation loss, which yielded about 120k, 110k, and 34k training steps with the learning rate of  $1e-4$  for MIMIC-IV, eICU, and HiRID, respectively. As a result, we trained the model for approximately 96, 92, and 72 hours with 2 A6000 48GB GPUs for each dataset, respectively.

**Naive** If no prior measurement exists for the target lab test within the corresponding ICU record, the prediction is set to the mean of that lab test’s values computed across the training set.

**Naive( $\mu$ )** If no prior measurements exist, the prediction defaults to the mean of that lab test’s values across the training set, similar to the Naive method.

**GenHPF** GenHPF has a hierarchical architecture consisting of an event encoder and an event aggregator, designed to perform multiple predictive tasks in a single framework. To adapt it for regressing multiple lab test outcomes, we construct samples by grouping the original samples that have the same prior medical history (*i.e.*, lab test samples that occurred at the same timestamp). Then, we manipulate the GenHPF model to regress every single lab test outcome given a sequence of medical events but compute the Mean Squared Error (MSE) loss only for the observed lab items for which we can define the ground-truth labels. Here, since lab items with large magnitudes may disproportionately influence the model training, we standardize the outcome values for each lab item using the mean and standard deviation computed from the training set. We maintain GenHPF’s core architecture, with key hyperparameters including a prediction dimension of 128, an embedding dimension of 128, 4 attention heads, and 2 transformer layers. Similar to LabTOP, we applied early stopping with the patience of 5 epochs based on the validation loss, which resulted in about 83k, 210k, and 71k training steps with the learning rate of  $3e-4$  for each dataset, respectively. As a result, we trained the model for approximately 39, 67, and 30 hours with a single 80GB A100 GPU for each respective dataset.

**XGBoost** For XGBoost, the input features include the count, mean, min, and max values for all medical items used in the dataset, which are treated as separate columns. As a result, the input consists of an array of the statistical summaries (count, mean, min, and max) of the unique events that precede the prediction time for the target lab item. We trained this model for each lab item existed in the dataset with a learning rate of 0.1, a maximum depth of 5, and 100 estimators.

**GPT-4o, GPT-4o-mini, and LLaMA-3.1-Instruct (8B)** To create samples for these LLMs<sup>5</sup>, we followed the same strategy with GenHPF. In other words, we grouped test samples that have the same prior medical history (*i.e.*, the lab items that occurred at the same time), and the LLM was instructed to answer values of the target lab items based on their prior sequence of medical events as prompt. The prompt we used for lab test outcome prediction can be found in Figure 3.

4. [https://huggingface.co/docs/transformers/model\\_doc/gpt2#transformers.GPT2LMHeadModel](https://huggingface.co/docs/transformers/model_doc/gpt2#transformers.GPT2LMHeadModel)

5. Specifically, at the time of the experiments, GPT-4o referred to gpt-4o-2024-11-20 and GPT-4o-mini corresponded to gpt-4o-mini-2024-07-18.

You are an AI model that predicts lab test values based on ICU medical history. Given a series of medical events recorded in the ICU (provided in the "Prompt"), predict the most likely value for each specified lab item at the last recorded time.

Use medical knowledge and reasonable assumptions based on typical ICU patient trends. The names of lab items are separated with |endofevent|. Each output of item should follow the format: <value> |endofevent|

Ensure that the predicted lab values are presented in the exact order in which the lab items appear in the Question section.

[Prompt Begin]  
[medical history]  
[Prompt End]

Question:  
[list of target lab items]

Output:

Figure 3: Template prompt used for GPT-4o and GPT-4o-mini. Note that [medical history] refers to the textual sequence of the test sample.

## Appendix C. Additional Experimental Results

**Performances by the time interval to the last measured time for the target lab test** To further illustrate the performance of our models and Naive model from another perspective, we conduct an additional analysis by grouping test set samples based on the time interval between the last measured time and the prediction time for the target lab item. Specifically, we categorized samples by whether the time interval to the last measured time for the target lab item is within 24 hours or not, and measured performances within each group. The results are shown in Table 13.

We observe that when the time interval between the last lab measurement and the prediction time is more than 24 hours, the performance gap between LabTOP and Naive becomes more significant. Since the Naive model directly copies the last observed value as the prediction, its performance remains relatively strong when lab values are measured frequently and do not change dynamically over short time spans. However, in longer time interval cases,

where patient conditions may have changed significantly, the Naive model struggles while LabTOP maintains higher predictive accuracy (SMAPE). This result suggests that more computationally advanced methods like LabTOP are particularly valuable in clinically meaningful scenarios, where lab tests are infrequent and accurate forecasting is essential for early detection and intervention. Therefore, while the computational cost of LabTOP is higher, this trade-off is necessary to achieve reliable performance in challenging clinical cases.

### LabTOP performances for individual lab items

The experimental results of LabTOP for each individual lab item in MIMIC-IV, eICU, and HiRID are presented in Table 10, Table 11, and Table 12, respectively.

### Model performances for normal and abnormal range values in MIMIC-IV

We group each lab test sample in the test split into normal and abnormal ranges using reference ranges provided in MIMIC-IV, and evaluate models separately for each group. These results are provided in Table 14.

### Exploration of different model configurations

We evaluate LabTOP’s performance at different model scales by varying the number of Transformer decoder layers, attention heads, and hidden dimension size. Specifically, we experiment with configurations comparable to BERT-mini, BERT-small, and BERT-base to analyze the effect of model size. The results of these experiments are presented in Table 15.

**Attention Map Analysis** To gain deeper insights into the prediction process of LabTOP, we can analyze an attention map to see how the model weighs different past clinical events when predicting a specific lab value. Here, since attention scores are generated for each predicted token across multiple layers and heads, these scores are systematically aggregated to construct a comprehensive attention representation for lab test outcome prediction. For each layer, the mean attention scores across all heads are computed, and these head-level averaged scores are then used to calculate the mean attention score for each layer. The aggregated attention score at each layer level is defined as:

$$A_{\text{final}} = \frac{1}{L} \sum_{l=1}^L \left( \frac{1}{H} \sum_{h=1}^H A_h^{(l)} \right) \quad (8)$$

where  $A_{\text{final}}$  represents the final aggregated attention score,  $L$  is the total number of layers,  $H$  is the total number of attention heads, and  $A_h^{(l)}$  denotes the attention score of head  $h$  in layer  $l$ . By averaging the attention maps computed for each predicted token, the final aggregated attention score is obtained. This resulting attention map captures attention scores from all preceding tokens before the target lab event.

To analyze attention at the event level, tokens before the target lab event are grouped based on their corresponding events. The total attention score for each event is computed by summing the attention scores of all tokens associated with that event. Event-level attention scores are then visualized to determine which past events are most influential in predicting the lab test outcome.

Figure 4 illustrates the aggregated attention map during the prediction of a glucose outcome. The glucose level in the preceding events is recorded as 103.0 mg/dL. The model assigned a relatively high attention score to insulin-regular, which is the key factor in predicting a subsequent decrease in glucose levels. Since both the model prediction and actual glucose measurement confirmed this decrease, the

analysis validates that the model effectively leverages relevant prior events to generate accurate predictions.

Table 6: Lab items included in each dataset (MIMIC-IV, eICU, and HiRID)

Dataset	Lab Items
MIMIC-IV (44 items)	glucose, potassium, sodium, chloride, ph, hemoglobin, hematocrit, bicarbonate, creatinine, anion gap, urea nitrogen, magnesium, phosphate, calcium, total, platelet count, white blood cells, mchc, red blood cells, mcv, mch, rdw, po2, base excess, calculated total co2, pco2, ptt, pt, inr(pt), h, l, i, lactate, rdw-sd, free calcium, oxygen saturation, potassium, whole blood, asparate aminotransferase (ast), bilirubin, total, alanine aminotransferase (alt), alkaline phosphatase, temperature, lactate dehydrogenase (ld), albumin, lymphocytes
eICU (41 items)	bedside glucose, potassium, sodium, glucose, hgb, chloride, creatinine, bun, hct, calcium, bicarbonate, platelets x 1000, wbc x 1000, rbc, mcv, mchc, mch, rdw, anion gap, magnesium, mpv, -lymphs, -monos, pao2, paco2, ph, hco3, fio2, -eos, phosphate, -polys, -basos, albumin, o2 sat (%), base excess, ast (sgot), total protein, alt (sgpt), alkaline phos., total bilirubin, pt - inr
HiRID (27 items)	glucose [moles/volume] in serum or plasma, sodium [moles/volume] in blood, potassium [moles/volume] in blood, bicarbonate [moles/volume] in arterial blood, base excess in arterial blood by calculation, oxygen saturation in arterial blood, methemoglobin/hemoglobin.total in arterial blood, carboxyhemoglobin/hemoglobin.total in arterial blood, calcium.ionized [moles/volume] in blood, lactate [mass/volume] in arterial blood, chloride [moles/volume] in blood, ph of arterial blood, hemoglobin [mass/volume] in arterial blood, oxygen [partial pressure] in arterial blood, carbon dioxide [partial pressure] in arterial blood, hemoglobin [mass/volume] in blood, leukocytes [# /volume] in blood, mcv [entitic volume], mch [entitic mass], mchc [mass/volume] in cord blood, platelets [# /volume] in blood, inr in blood by coagulation assay, creatinine [moles/volume] in blood, c reactive protein [mass/volume] in serum or plasma, urea [moles/volume] in venous blood, phosphate [moles/volume] in blood, magnesium [moles/volume] in blood

Table 7: Time intervals for each lab item in MIMIC-IV

Item	Time Interval (Hours)
Alanine Aminotransferase (ALT)	25.65
Albumin	40.22
Alkaline Phosphatase	25.79
Anion Gap	13.38
Aspartate Aminotransferase (AST)	25.62
Base Excess	7.63
Bicarbonate	13.34
Bilirubin, Total	25.53
Calcium, Total	14.09
Calculated Total CO2	7.63
Chloride	12.79
Creatinine	13.40
Free Calcium	10.33
Glucose	9.99
H	10.94
Hematocrit	13.26
Hemoglobin	12.80
I	10.94
INR (PT)	18.41
L	10.94
Lactate	10.98
Lactate Dehydrogenase (LD)	33.55
Lymphocytes	47.93
Magnesium	13.45
MCH	15.05
MCHC	15.05
MCV	15.05
Oxygen Saturation	9.34
PCO2	7.63
pH	7.85
Phosphate	14.00
Platelet Count	14.74
PO2	7.62
Potassium	12.43
Potassium, Whole Blood	9.93
PT	18.41
PTT	16.25
RDW	15.06
RDW-SD	14.41
Red Blood Cells	15.05
Sodium	12.42
Temperature	17.91
Urea Nitrogen	13.44
White Blood Cells	15.04
<b>Average</b>	<b>15.80</b>

Table 8: Time intervals for each lab item in eICU

Item	Time Interval (Hours)
Basos	25.80
Eos	25.78
Lymphs	24.57
Monos	24.60
Polys	24.85
Albumin	26.75
Alkaline Phos.	28.56
ALT (SGPT)	28.67
Anion Gap	17.54
AST (SGOT)	28.62
Base Excess	14.68
Bedside Glucose	4.10
Bicarbonate	17.44
BUN	17.57
Calcium	17.63
Chloride	17.29
Creatinine	17.53
FiO2	14.65
Glucose	16.64
HCO3	14.13
Hct	17.34
Hgb	16.82
Magnesium	20.06
MCH	20.21
MCHC	20.19
MCV	20.18
MPV	20.36
O2 Sat (%)	14.34
PaCO2	13.89
PaO2	13.91
pH	13.87
Phosphate	21.55
Platelets $\times 1000$	19.97
Potassium	14.10
PT - INR	24.72
RBC	20.24
RDW	20.31
Sodium	15.43
Total Bilirubin	28.46
Total Protein	28.62
WBC $\times 1000$	20.24
<b>Average</b>	<b>19.81</b>

Table 9: Time intervals for each lab item in HiRID

Item	Time Interval (Hours)
Base Excess in Arterial Blood by Calculation	6.59
Bicarbonate [moles/volume] in Arterial Blood	6.59
C-Reactive Protein [mass/volume] in Serum or Plasma	24.72
Calcium, Ionized [moles/volume] in Blood	6.59
Carbon Dioxide [partial pressure] in Arterial Blood	6.41
Carboxyhemoglobin/Hemoglobin Total in Arterial Blood	6.58
Chloride [moles/volume] in Blood	6.64
Creatinine [moles/volume] in Blood	23.74
Glucose [moles/volume] in Serum or Plasma	3.85
Hemoglobin [mass/volume] in Arterial Blood	6.39
Hemoglobin [mass/volume] in Blood	17.67
INR in Blood by Coagulation Assay	21.09
Lactate [mass/volume] in Arterial Blood	6.68
Leukocytes [# /volume] in Blood	18.26
Magnesium [moles/volume] in Blood	26.61
MCH [entitic mass]	18.35
MCHC [mass/volume] in Cord Blood	18.35
MCV [entitic volume]	18.32
Methemoglobin/Hemoglobin Total in Arterial Blood	6.57
Oxygen [partial pressure] in Arterial Blood	6.39
Oxygen Saturation in Arterial Blood	6.57
pH of Arterial Blood	6.31
Phosphate [moles/volume] in Blood	24.72
Platelets [# /volume] in Blood	18.74
Potassium [moles/volume] in Blood	6.82
Sodium [moles/volume] in Blood	6.77
Urea [moles/volume] in Venous Blood	24.43
<b>Average</b>	<b>12.99</b>

Table 10: LabTOP performance for each individual lab item in MIMIC-IV

Item	Count	MAE	SMAPE	Unit
Glucose	72887	48.81 $\pm$ 2.39	20.04 $\pm$ 0.44	mg/dL
Sodium	60140	1.40 $\pm$ 1.09	3.27 $\pm$ 3.64	mEq/L
Potassium	60131	0.84 $\pm$ 1.08	5.12 $\pm$ 3.64	mEq/L
Ph	59069	0.20 $\pm$ 0.06	2.69 $\pm$ 0.18	units
Chloride	59000	2.12 $\pm$ 0.01	2.06 $\pm$ 0.01	mEq/L
Hemoglobin	57786	0.65 $\pm$ 0.00	6.72 $\pm$ 0.03	g/dL
Bicarbonate	56749	1.61 $\pm$ 0.00	6.83 $\pm$ 0.00	mEq/L
Hematocrit	56497	1.88 $\pm$ 0.00	6.33 $\pm$ 0.01	%
Anion Gap	56445	1.79 $\pm$ 0.01	13.18 $\pm$ 0.06	mEq/L
Urea Nitrogen	56406	4.32 $\pm$ 0.01	15.84 $\pm$ 0.03	mg/dL
Creatinine	56086	0.22 $\pm$ 0.04	13.62 $\pm$ 0.06	mg/dL
Magnesium	54857	0.13 $\pm$ 0.01	6.29 $\pm$ 0.01	mg/dL
Phosphate	52445	0.51 $\pm$ 0.00	14.71 $\pm$ 0.04	mg/dL
Calcium, Total	51933	0.32 $\pm$ 0.03	3.57 $\pm$ 0.02	mg/dL
Platelet Count	51197	29.21 $\pm$ 0.21	16.73 $\pm$ 0.15	K/uL
Po2	50431	31.6 $\pm$ 0.16	26.81 $\pm$ 0.25	mm Hg
Base Excess	50431	1.33 $\pm$ 0.00	65.21 $\pm$ 0.51	mEq/L
Pco2	50379	4.23 $\pm$ 0.01	9.76 $\pm$ 0.03	mm Hg
Calculated Total Co2	50329	1.42 $\pm$ 0.01	5.72 $\pm$ 0.01	mEq/L
White Blood Cells	50194	2.27 $\pm$ 0.01	19.75 $\pm$ 0.22	K/uL
Red Blood Cells	50153	0.22 $\pm$ 0.0	6.71 $\pm$ 0.01	m/uL
Mch	50122	0.65 $\pm$ 0.01	2.19 $\pm$ 0.01	pg
Rdw	50109	0.51 $\pm$ 0.01	3.22 $\pm$ 0.04	%
Mchc	50066	0.64 $\pm$ 0.0	1.96 $\pm$ 0.01	%, g/dL
Mcv	50045	1.70 $\pm$ 0.01	1.85 $\pm$ 0.01	g/dL
Ptt	37743	8.95 $\pm$ 0.24	15.43 $\pm$ 0.36	sec
Inr ( Pt )	34670	0.18 $\pm$ 0.01	10.36 $\pm$ 0.14	None
Pt	34659	1.98 $\pm$ 0.02	10.14 $\pm$ 0.10	sec
L	32700	5.69 $\pm$ 0.02	37.54 $\pm$ 0.14	U
Lactate	31327	0.55 $\pm$ 0.00	23.28 $\pm$ 0.28	mmol/L
H	30831	11.41 $\pm$ 0.31	104.29 $\pm$ 7.62	U
Rdw - Sd	29442	1.93 $\pm$ 0.02	3.61 $\pm$ 0.04	fL
Free Calcium	28758	0.05 $\pm$ 0.0	4.27 $\pm$ 0.07	mmol/L
I	25471	0.32 $\pm$ 0.0	17.09 $\pm$ 0.22	U
Oxygen Saturation	18239	9.31 $\pm$ 0.16	12.37 $\pm$ 0.30	%
Potassium, Whole Blood	16293	0.32 $\pm$ 0.04	7.08 $\pm$ 0.01	mEq/L
Asparate Aminotransferase ( Ast )	14980	81.23 $\pm$ 0.79	43.65 $\pm$ 0.39	IU/L
Alkaline Phosphatase	14696	31.38 $\pm$ 0.18	23.61 $\pm$ 0.12	IU/L
Alanine Aminotransferase ( Alt )	14582	53.34 $\pm$ 0.34	44.77 $\pm$ 0.68	IU/L
Bilirubin, Total	13902	0.70 $\pm$ 0.01	34.28 $\pm$ 0.23	mg/dL
Temperature	10331	0.47 $\pm$ 0.02	1.29 $\pm$ 0.02	°C
Lactate Dehydrogenase ( Ld )	8792	177.57 $\pm$ 2.22	29.48 $\pm$ 0.21	IU/L
Albumin	7552	0.31 $\pm$ 0.01	10.69 $\pm$ 0.11	g/dL
Lymphocytes	7488	7.00 $\pm$ 0.18	70.41 $\pm$ 3.78	%

Table 11: LabTOP performance for each individual lab item in eICU

Item	Count	MAE	SMAPE	Unit
Bedside Glucose	179312	22.83 $\pm$ 1.78	15.16 $\pm$ 0.03	mg/dL
Potassium	77648	0.32 $\pm$ 0.00	8.08 $\pm$ 0.02	mmol/L
Sodium	71184	2.22 $\pm$ 0.01	1.62 $\pm$ 0.03	mmol/L
Glucose	67292	22.53 $\pm$ 0.02	15.58 $\pm$ 0.01	mg/dL
Hgb	65241	0.84 $\pm$ 0.03	8.03 $\pm$ 0.02	g/dL
Chloride	64786	2.53 $\pm$ 0.01	2.44 $\pm$ 0.01	mmol/L
Creatinine	64094	0.29 $\pm$ 0.00	18.90 $\pm$ 0.02	mg/dL
Hct	63676	2.43 $\pm$ 0.01	7.95 $\pm$ 0.04	%
Bun	63539	5.98 $\pm$ 0.02	22.59 $\pm$ 0.03	mg/dL
Calcium	61862	0.33 $\pm$ 0.00	4.04 $\pm$ 0.01	mg/dL
Bicarbonate	61027	1.94 $\pm$ 0.01	8.10 $\pm$ 0.01	mmol/L
Platelets X 1000	56096	34.39 $\pm$ 0.1	19.33 $\pm$ 0.02	K/mcL
Wbc X 1000	55922	2.70 $\pm$ 0.01	23.17 $\pm$ 0.08	K/mcL
Rbc	55748	0.29 $\pm$ 0.01	8.19 $\pm$ 0.01	M/mcL
Mcv	54438	2.16 $\pm$ 0.33	2.23 $\pm$ 0.01	fL
Mchc	54131	0.63 $\pm$ 0.00	1.93 $\pm$ 0.01	g/dL
Mch	51772	0.75 $\pm$ 0.01	2.55 $\pm$ 0.01	pg
Rdw	51522	0.68 $\pm$ 0.01	4.27 $\pm$ 0.02	%
Anion Gap	50748	1.98 $\pm$ 0.01	20.21 $\pm$ 0.02	nan
Magnesium	38416	0.20 $\pm$ 0.03	9.61 $\pm$ 0.01	mg/dL
Mpv	37782	0.48 $\pm$ 0.00	4.90 $\pm$ 0.01	fL
Pao2	29405	35.90 $\pm$ 0.14	29.50 $\pm$ 0.05	mm Hg
Paco2	29181	5.46 $\pm$ 0.01	12.75 $\pm$ 0.02	mm Hg
Ph	28965	0.07 $\pm$ 0.03	0.67 $\pm$ 0.03	nan
Monos	28891	2.69 $\pm$ 0.01	46.81 $\pm$ 0.06	%
Lymphs	28774	4.64 $\pm$ 0.14	46.58 $\pm$ 0.01	%
Hco3	27738	1.89 $\pm$ 0.01	8.18 $\pm$ 0.02	mmol/L
Phosphate	26150	0.67 $\pm$ 0.00	20.53 $\pm$ 0.03	mg/dL
Polys	25945	6.63 $\pm$ 0.01	9.43 $\pm$ 0.03	%
Fio2	23978	10.51 $\pm$ 0.04	24.87 $\pm$ 0.10	%
Albumin	23545	0.28 $\pm$ 0.00	10.58 $\pm$ 0.03	g/dL
Base Excess	23264	2.37 $\pm$ 0.35	75.72 $\pm$ 0.11	mEq/L
O2 Sat ( % )	21639	2.89 $\pm$ 0.01	3.14 $\pm$ 0.01	%
Ast ( Sgot )	20840	86.46 $\pm$ 0.95	52.92 $\pm$ 0.13	Units/L
Total Protein	20677	0.43 $\pm$ 0.01	7.48 $\pm$ 0.01	g/dL
Alt ( Sgpt )	20529	54.60 $\pm$ 0.98	46.49 $\pm$ 0.29	Units/L
Alkaline Phos.	20391	25.44 $\pm$ 0.14	23.59 $\pm$ 0.03	Units/L
Total Bilirubin	19399	0.53 $\pm$ 0.01	38.07 $\pm$ 0.13	mg/dL
Pt - Inr	18298	0.30 $\pm$ 0.01	16.27 $\pm$ 0.08	ratio
Eos	17160	1.22 $\pm$ 0.01	107.39 $\pm$ 0.21	%
Basos	10767	0.31 $\pm$ 0.00	92.78 $\pm$ 0.17	%

Table 12: LabTOP performance for each individual lab item in HiRID

Item	Count	MAE	SMAPE	Unit
Glucose [ Moles / Volume ] In Serum Or Plasma	45573	1.28 $\pm$ 0.01	15.40 $\pm$ 0.05	mmol/L
Sodium [ Moles / Volume ] In Blood	24856	1.72 $\pm$ 0.01	1.26 $\pm$ 0.01	mmol/L
Potassium [ Moles / Volume ] In Blood	24587	0.26 $\pm$ 0.00	6.27 $\pm$ 0.02	mmol/L
Bicarbonate [ Moles / Volume ] In Arterial Blood	22615	1.32 $\pm$ 0.01	5.69 $\pm$ 0.05	mmol/L
Base Excess In Arterial Blood By Calculation	22582	1.46 $\pm$ 0.01	74.43 $\pm$ 0.92	mmol/L
Calcium. Ionized [ Moles / Volume ] In Blood	22396	0.03 $\pm$ 0.00	2.92 $\pm$ 0.01	mmol/L
Carboxyhemoglobin / Hemoglobin. Total In Arterial Blood	22389	0.27 $\pm$ 0.00	21.14 $\pm$ 0.07	%
Methemoglobin / Hemoglobin. Total In Arterial Blood	22346	0.27 $\pm$ 0.00	31.81 $\pm$ 0.21	%
Lactate [ Mass / Volume ] In Arterial Blood	22321	0.50 $\pm$ 0.00	26.95 $\pm$ 0.17	mmol/L
Chloride [ Moles / Volume ] In Blood	21994	1.88 $\pm$ 0.01	1.73 $\pm$ 0.02	mmol/L
Oxygen Saturation In Arterial Blood	21781	1.57 $\pm$ 0.05	1.59 $\pm$ 0.02	%
Hemoglobin [ Mass / Volume ] In Arterial Blood	20697	6.19 $\pm$ 0.05	6.10 $\pm$ 0.09	g/L
Ph Of Arterial Blood	20673	0.03 $\pm$ 0.00	0.43 $\pm$ 0.01	None
Oxygen [ Partial Pressure ] In Arterial Blood	20586	22.02 $\pm$ 0.30	20.11 $\pm$ 0.11	mmHg
Carbon Dioxide [ Partial Pressure ] In Arterial Blood	20313	3.38 $\pm$ 0.01	9.20 $\pm$ 0.04	mmHg
Hemoglobin [ Mass / Volume ] In Blood	10373	6.02 $\pm$ 0.08	5.94 $\pm$ 0.07	g/L
Leukocytes [ # / Volume ] In Blood	10124	3.12 $\pm$ 0.04	28.34 $\pm$ 0.09	G/L
Mchc [ Mass / Volume ] In Cord Blood	10037	6.59 $\pm$ 0.09	1.95 $\pm$ 0.02	g/L
Mcv [ Entitic Volume ]	10016	2.93 $\pm$ 0.04	3.19 $\pm$ 0.01	fL
Mch [ Entitic Mass ]	9992	1.12 $\pm$ 0.00	3.62 $\pm$ 0.02	pg
Platelets [ # / Volume ] In Blood	9794	59.81 $\pm$ 0.63	39.99 $\pm$ 0.11	G/L
Creatinine [ Moles / Volume ] In Blood	7424	35.31 $\pm$ 1.20	29.87 $\pm$ 0.35	umol/L
C Reactive Protein [ Mass / Volume ] In Serum or Plasma	6834	66.40 $\pm$ 1.20	84.87 $\pm$ 0.53	mg/L
Urea [ Moles / Volume ] In Venous Blood	6248	3.64 $\pm$ 0.06	35.26 $\pm$ 0.28	mmol/L
Inr In Blood By Coagulation Assay	6010	0.16 $\pm$ 0.00	12.10 $\pm$ 0.41	None
Phosphate [ Moles / Volume ] In Blood	5385	0.26 $\pm$ 0.00	23.23 $\pm$ 0.24	mmol/L
Magnesium [ Moles / Volume ] In Blood	5195	0.12 $\pm$ 0.00	12.85 $\pm$ 0.02	mmol/L

Table 13: Lab test outcome prediction performances of LabTOP and Naive on MIMIC-IV, aggregated by whether the interval to the last measured time for the target lab test is within 24 hours or not

	<24h	$\geq 24h$
<b><i>NMAE</i></b>		
Naive	0.072	0.076
LabTOP	0.054 $\pm$ 0.000	0.051 $\pm$ 0.000
<b><i>SMAPE (%)</i></b>		
Naive	15.91	20.39
LabTOP	12.46 $\pm$ 0.23	12.44 $\pm$ 0.21

Table 14: Lab test outcome prediction performances for normal-range and abnormal-range samples in MIMIC-IV. The best performances for each category (Normal, Abnormal) are highlighted with **boldface**.

	Normal	Abnormal
<b><i>NMAE</i></b>		
Naive	0.081	0.104
Naive( $\mu$ )	0.093	0.131
GenHPF	0.099 $\pm$ 0.015	0.132 $\pm$ 0.012
XGBoost	0.070	0.105
GPT-4o	0.196	0.209
GPT-4o-mini	0.805	0.738
LLaMA-3.1-Inst.	1.340	1.115
<b>LabTOP</b>	<b>0.051<math>\pm</math>0.001</b>	<b>0.084<math>\pm</math>0.001</b>
<b><i>SMAPE (%)</i></b>		
Naive	16.94	17.80
Naive( $\mu$ )	19.80	19.30
GenHPF	26.42 $\pm$ 0.92	26.52 $\pm$ 3.08
XGBoost	22.61	23.45
GPT-4o	20.81	22.92
GPT-4o-mini	41.90	46.11
LLaMA-3.1-Inst.	71.74	79.64
<b>LabTOP</b>	<b>15.25<math>\pm</math>0.41</b>	<b>17.58<math>\pm</math>0.16</b>

Table 15: Lab test outcome prediction performances of LabTOP with different model configurations. Note that LabTOP-base is used by default for all the experiments in this paper.

Model	Layers	Attention Heads	Hidden Dimension	Parameter Size	NMAE	SMAPE
LabTOP-mini	4	4	256	11M	0.069 $\pm$ 0.003	16.02 $\pm$ 0.53
LabTOP-small	4	8	512	30M	0.067 $\pm$ 0.005	16.24 $\pm$ 1.28
LabTOP-base	12	8	512	53M	0.064 $\pm$ 0.001	14.80 $\pm$ 0.13
LabTOP-large	12	12	768	110M	0.063 $\pm$ 0.003	15.06 $\pm$ 0.62

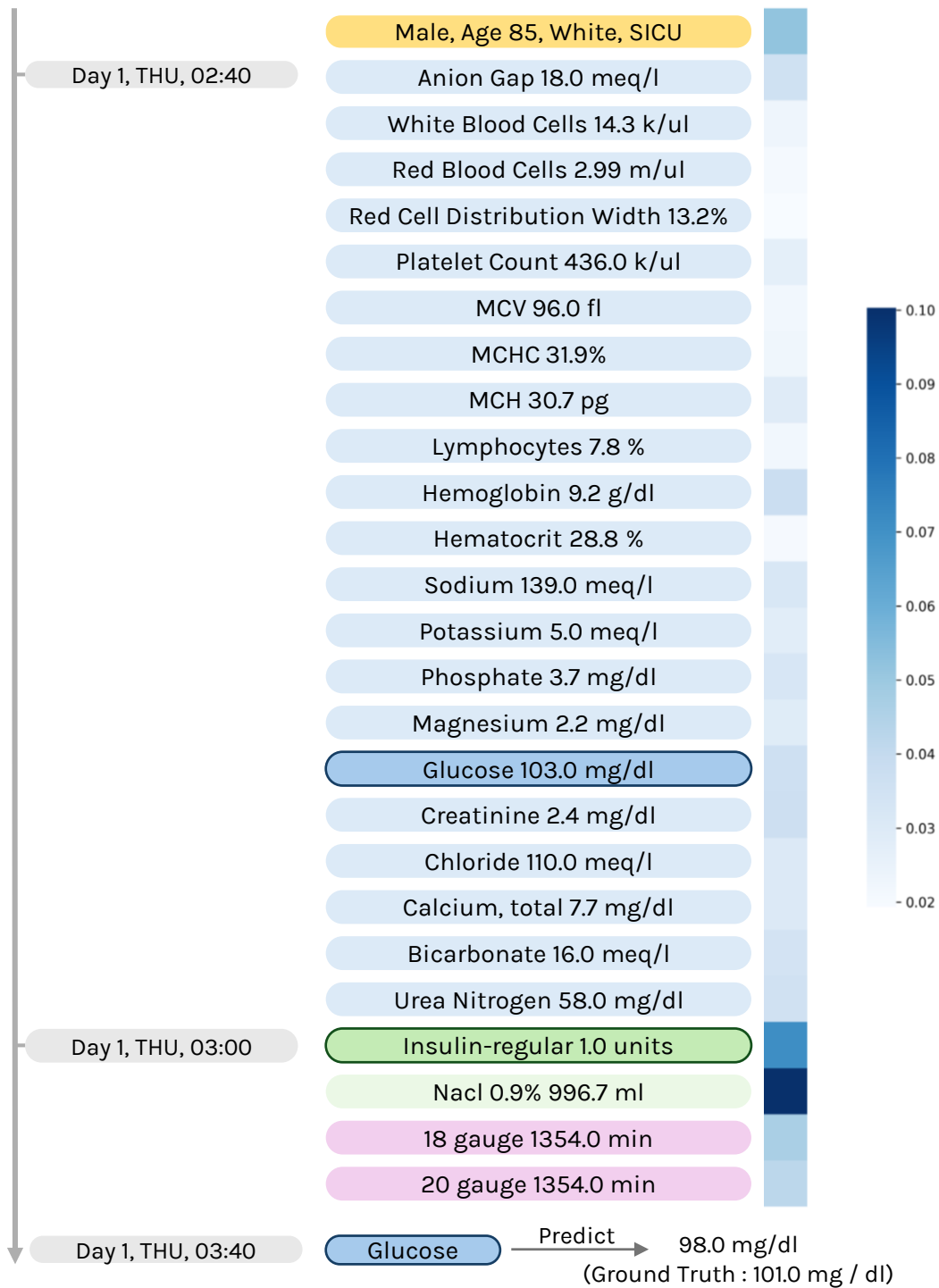


Figure 4: An example of an attention map for LabTOP computed when predicting the glucose outcome